



# LncRNA XIST knockdown ameliorates oxidative low-density lipoprotein-induced endothelial cells injury by targeting miR-204-5p/TLR4

GUOYONG LU<sup>1,2</sup>, PENG TIAN<sup>1,2</sup>, YONGXIN ZHU<sup>1,2</sup>, XIAOHUA ZUO<sup>1,2</sup> and XIAOQIANG LI<sup>3\*</sup>

<sup>1</sup>Department of Vascular Surgery, The Huaian Hospital Affiliated to Xuzhou Medical University, Huai'an, Jiangsu, China

<sup>2</sup>Department of Vascular Surgery, The Second People's Hospital of Huai'an, Huai'an, Jiangsu, China

<sup>3</sup>Department of Vascular Surgery, Nanjing Drum Tower Hospital Affiliated to Nanjing University Medical School, Nanjing, Jiangsu, China

\*Corresponding author (Email, f2869082tuhuan386@163.com)

MS received 10 June 2019; accepted 2 March 2020; published online 25 March 2020

Oxidative low-density lipoprotein (ox-LDL)-induced endothelial cell injury is a key contributor to atherosclerosis development. However, the role and mechanism of long noncoding RNA X-inactive specific transcript (XIST) in atherosclerosis remain largely unknown. The ox-LDL-induced human umbilical vein endothelial cells (HUVECs) injury was analyzed by cell viability, apoptosis, inflammatory cytokines secretion and oxidative stress. The expression levels of XIST, microRNA-204-5p (miR-204-5p) and toll-like receptor 4 (TLR4) were detected by quantitative real-time polymerase chain reaction and western blot, respectively. The target interaction between miR-204-5p and XIST or TLR4 was explored by bioinformatics analysis, luciferase assay and RNA immunoprecipitation. The expression of XIST was enhanced in ox-LDL-treated HUVECs. Knockdown of XIST attenuated ox-LDL-induced viability inhibition, apoptosis production, inflammatory response and oxidative stress in HUVECs. XIST was validated as a sponge of miR-204-5p and TLR4 acted as a target of miR-204-5p. Knockdown of miR-204-5p reversed silence of XIST-mediated suppressive role in ox-LDL-induced injury. TLR4 alleviated miR-204-5p-mediated inhibitive effect on ox-LDL-induced injury. Moreover, XIST could regulate TLR4 expression by sponging miR-204-5p. In conclusion, silence of XIST displayed a protective role in ox-LDL-induced injury in HUVECs by regulating miR-204-5p/TLR4 axis, providing a novel mechanism for understanding the pathogenesis of atherosclerosis.

**Keywords.** Atherosclerosis; ox-LDL; HUVECs; XIST; miR-204-5p; TLR4

**Abbreviations:** ELISA, enzyme-linked immunosorbent assay; HUVECs, human umbilical vein endothelial cells; lncRNAs, long noncoding RNAs; ox-LDL, oxidative low-density lipoprotein; qRT-PCR, quantitative real-time polymerase chain reaction; RIP, RNA immunoprecipitation; TLR4, toll-like receptor 4; XIST, X-inactive specific transcript

## 1. Introduction

Atherosclerosis is one chronic inflammatory vascular disorder with the leading cause of mortality and morbidity worldwide (Pothineni *et al.* 2017). Oxidative

stress and inflammatory response are two key processes participating in the development of atherosclerosis (Yuan *et al.* 2019). Endothelial cells play essential roles in vascular function and the cell dysfunction is regarded as a crucial marker for atherosclerosis (Haybar

*Electronic supplementary material:* The online version of this article (<https://doi.org/10.1007/s12038-020-0022-0>) contains supplementary material, which is available to authorized users.

*et al.* 2019). Oxidative low-density lipoprotein (ox-LDL) is an important risk factor of cardiovascular diseases including atherosclerosis and it could induce endothelial dysfunction (Trpkovic *et al.* 2015). However, the mechanisms and effective therapeutics for atherosclerosis are limited.

Noncoding RNAs, including long noncoding RNAs (lncRNAs) and microRNAs (miRNAs), are implicated in the regulation of endothelial function in the pathogenesis of atherosclerosis (Aryal and Suarez 2019). LncRNAs are described as sequences longer than 200 nucleotides, which are associated with ox-LDL-induced endothelial dysfunction (Singh *et al.* 2017). Previous studies have reported that lncRNAs such as metastasis-associated lung adenocarcinoma transcript 1 and growth-arrest specific transcript 5 could serve as competitive endogenous RNAs (ceRNAs) to regulate ox-LDL-induced inflammatory response and cell apoptosis in endothelial cells during atherosclerosis (Li *et al.* 2018; Liang *et al.* 2019). LncRNA X-inactive specific transcript (XIST) has been suggested to play promoting roles in human cancers and diseases (Liu *et al.* 2019; Wei *et al.* 2019). The previous studies display that XIST could take part in the regulation of endothelial injury under hypoxia (Fasanaro *et al.* 2009; Neumann *et al.* 2018). Hence, we hypothesized that XIST might be likely to play an important role in endothelial dysfunction. Moreover, the emerging evidence indicates that XIST could promote ox-LDL-induced endothelial injury during atherosclerosis (Xu *et al.* 2018). However, the potential mechanism by which XIST mediates atherosclerosis progression remains largely unclear.

As one class of noncoding RNAs with 18-24 nucleotides, miRNAs have essential roles in the development and therapeutics of cardiovascular diseases, including atherosclerosis (Islas and Moreno-Cuevas 2018). Former work has demonstrated the protective role of miR-204 in ox-LDL-induced atherosclerosis (Yan *et al.* 2019). Nevertheless, little is known about the role of its mature miR-204-5p in atherosclerosis. Toll-like receptors (TLRs), such as TLR2, TLR4, TLR7 and TLR9, play pivotal roles in the prevention and treatment of inflammatory diseases (Hennessy *et al.* 2010). More importantly, TLR4 has been reported as an important contributor to atherosclerosis (den Dekker *et al.* 2010). The sequences of XIST and TLR4 3' UTR contains the predicted binding sites of miR-204-5p. Hence, it possibly exists that XIST could regulate atherosclerosis progression by sponging miR-204-5p and regulating TLR4. In the current study, ox-LDL-challenged human umbilical vein endothelial cells (HUVECs) were used a cellular model of atherosclerosis *in vitro*. Using this model,

we investigated the effect of XIST on cell viability, apoptosis, inflammatory response and oxidative stress in HUVECs and explored the potential ceRNA network of XIST/miR-204-5p/TLR4.

## 2. Materials and methods

### 2.1 Cell culture and transfection

HUVECs were purchased from American Type Culture Collection (cat. no. CRL-1730, Manassas, VA, USA) and cultured at 37°C under 5% CO<sub>2</sub> in RPMI-1640 medium containing 10% fetal bovine serum (cat. no. 11875093, Gibco, Grand Island, NY, USA). The medium was changed every three days.

Small interfering RNA (siRNA) against XIST (si-XIST) (5'- GUAUCCUAUUUGCAGCUAdTdT-3'), siRNA against TLR4 (si-TLR4) (5'- UAAAACGG CAGCAUUUAGCAAAdTdT-3'), siRNA negative control (si-NC) (5'- UUCUCCGAACGUGUCACGdT dT-3'), pcDNA3.1-based XIST overexpression vector and pcDNA3.1-based TLR4 overexpression vector were generated from Genepharma (Shanghai, China). pcDNA3.1 empty vector (pcDNA) acted as a negative control. miR-204-5p mimic (cat. no. miR10000265-1-5) and miR-204-5p inhibitor (in-miR-204-5p) (cat. no. miR20000265-1-5) including their corresponding negative control (miR-NC, in-miR-NC) were purchased from Ribobio (Guangzhou, China). When reaching 60% confluence, HUVECs in 6-well plates were transfected with 25 nM oligonucleotides or 1 µg vectors using Lipofectamine 2000 (cat. no. 11668019, Invitrogen, Carlsbad, CA, USA) following the manufactures' instructions. After the transfection for 24 h, cells were harvested for subsequent analyses.

### 2.2 Cell viability

Cell viability was measured using MTT cytotoxicity assay kit (cat. no. C0009, Beyotime, Shanghai, China). HUVECs (1 × 10<sup>4</sup> cells/well) were seeded into 96-well plates in triplicate overnight. Cells were incubated with 25, 50 or 100 µg/ml ox-LDL (cat. no. 20605ES05, Yeasen, Shanghai, China) for 24 h, or treated with 50 µg/ml ox-LDL for 12, 24 or 48 h. The un-treated cells were regarded as control. At the ending point, the medium was changed with fresh medium containing 0.5 mg/ml MTT solution. After culture for another 4 h, 100 µl formazan dissolving solution was added to each well. Subsequently, the absorbance of each well at 570 nm

was determined using a microplate reader (Bio-Rad, Hercules, CA, USA) and cell viability was expressed as the percentage of viability relative to control group.

### 2.3 Flow cytometry

Annexin V-FITC/PI apoptosis detection kit (cat. no. C1062L, Beyotime) was used for cell apoptosis assay through flow cytometry. Transfected or non-transfected HUVECs ( $1 \times 10^5$  cells/well) were seeded into 6-well plates overnight, followed by incubation with 50  $\mu\text{g/ml}$  ox-LDL for 24 h. The un-treated cells were regarded as control. After the digestion and collection, cells were resuspended in binding buffer and then interacted in the dark with 5  $\mu\text{l}$  Annexin V-FITC and PI for 10 min. Cells were analyzed using a flow cytometer (Becton Dickinson, San Jose, CA, USA). The lower right quadrant represented apoptotic cells at early stage and the upper right quadrant represented apoptotic cells at advanced stage and necrotic cells. In this study, the apoptotic rate was expressed as the percentage of cells at lower and upper right quadrants.

Cell cycle distribution was determined via flow cytometry. After treatment of ox-LDL for 24 h,  $1 \times 10^6$  HUVECs were harvested and then fixed with 70% ethanol overnight. Next, cells were incubated with RNase A (cat. no. R1253, Thermo Fisher, Waltham, MA, USA) and dyed with PI. Cells at different phases (G0/G1, S or G2/M) were determined through a flow cytometer.

### 2.4 Enzyme-linked immunosorbent assay (ELISA)

Transfected or non-transfected HUVECs ( $5 \times 10^4$  cells/well) were seeded into 24-well plates and subjected to 50  $\mu\text{g/ml}$  ox-LDL for 24 h. Cells without the treatment of ox-LDL were used as control. Cell supernatants were collected for analyses of inflammatory cytokines secretion levels using specific commercial ELISA kits (Multi Science, Hangzhou, China) for tumor necrosis factor-alpha (TNF- $\alpha$ ) (cat. no. 70-EK182-96), interleukin-1 beta (IL-1 $\beta$ ) (cat. no. 70-EK101B-96) and IL-6 (cat. no. 70-EK106/2-96) according to the manufacturer's instructions. The absorbance at 450 nm was measured using a microplate reader and the results of ELISA were calculated on the basis of standard curve.

### 2.5 Oxidative stress assay

For oxidative stress assay, transfected or non-transfected HUVEC cells ( $1 \times 10^4$  cells/per well) were

seeded into 96-well plates and then stimulated with 50  $\mu\text{g/ml}$  ox-LDL for 24 h. Subsequently, cells were collected for analyses of intracellular ROS level, anti-oxidative enzyme superoxide dismutase (SOD) activity and malonaldehyde (MDA) content using Reactive Oxygen Species Assay kit (cat. no. S0033, Beyotime), Total Superoxide Dismutase Assay kit (cat. no. S0101, Beyotime) and Lipid Peroxidation MDA Assay kit (cat. no. S0131, Beyotime) respectively following the manufacturer's instructions. The oxidative stress was presented as percentage of controls.

### 2.6 Quantitative real-time polymerase chain reaction (qRT-PCR)

RNA was isolated from HUVECs using RNA isolation reagent (cat. no. E01010A, Fulengen, Guangzhou, China) following the manufacturer's protocols. The samples were reversely transcribed using All-in-One mRNA or miRNA first-strand cDNA synthesis kit (cat. no. AORT-0020 or QP013, Fulengen) and then used for qRT-PCR through All-in-One qPCR mix (cat. no. QP001, Fulengen). The primers generated by Sangon (Shanghai, China) were listed as follows: XIST (Forward, 5'- AAT GACTGACCACTGCTGGG-3'; Reverse, 5'- GTGTAG GTGGTTCCCAAGG-3'); TLR4 (Forward, 5'-AAGT TATTGTGGTGGTGTCTAG-3'; Reverse, 5'-GAGGTA GGTGTTTCTGCTAAG-3'); GAPDH (Forward, 5'- AG AAGGCTGGGGCTCATTTG-3'; Reverse, 5'- AGGGG CCATCCACAGTCTTC-3'). The primers for miR-204-5p (cat. no. HmiRQP0306) and U6 (cat. no. HmiRQP9001) were purchased from Fulengen. GAPDH and U6 were used as internal controls, respectively. The relative expression levels of XIST, miR-204-5p and TLR4 were calculated according to the  $2^{-\Delta\Delta\text{Ct}}$  method (Livak and Schmittgen 2001).

### 2.7 Bioinformatics analysis, luciferase assay and RNA immunoprecipitation (RIP)

Bioinformatics analysis was performed using DIANA tool (<http://diana.imis.athena-innovation.gr/DianaTools/index.php>), predicting the binding sites of miR-204-5p and XIST or TLR4. The sequences of XIST containing the putative binding sites of miR-204-5p (AAAGGGA) were amplified and cloned into pmirGLO vectors (cat. no. E1330, Promega, Madison, WI, USA) to generate wild-type luciferase reporter vector XIST WT. Its mutant (XIST MUT) was generated by mutating the seed sites to UUUCCCU using the Fast Site-Directed Mutagenesis Kit

(cat. no. KM101, Tiangen, Beijing, China). The pmirGLO vectors were also used to generate wild-type luciferase reporter vector TLR4 WT, which was mutated by changing the seed sites, named as TLR4 MUT. Luciferase assay was performed in HUVECs co-transfected with 200 ng wild-type or mutant luciferase reporter constructs and 25 nM miR-204-5p mimic or miR-NC using Lipofectamine 2000. Cells were harvested after 24 h, and a luciferase reporter assay kit (cat. no. E1910, Promega) was used for luciferase activity assay.

For RIP assay in HUVECs, the Magna RNA immunoprecipitation kit (cat. no. 17-700, Millipore, Billerica, MA, USA) was used. Cells transfected with miR-204-5p mimic or miR-NC were collected and lysed in RIP lysis buffer, followed by incubation with magnetic beads which were pre-coated with Ago2 antibody (cat. no. ab32381, Abcam, Cambridge, MA, USA). IgG (cat. no. AP112, Sigma, St. Louis, MO, USA) was used as control. qRT-PCR was performed to measure the XIST level enriched in the complex.

## 2.8 Western blot

Proteins were extracted from HUVECs using RIPA buffer with 1% PMSF (cat. no. P0013B, Beyotime) and quantified using BCA Protein Assay kit (cat. no. P0012S, Beyotime). Samples were subjected to SDS-PAGE and transferred to PVDF membranes (cat. no. ISEQ00010, Millipore). After blocking the nonspecific binding sites using 5% non-fat milk, the membranes were incubated with the indicated primary antibodies overnight at 4°C and then interacted with secondary antibodies for 2 h. The anti-TLR4 (cat. no. ab217274), anti- $\beta$ -actin (cat. no. ab227387) and corresponding secondary antibody (cat. no. ab205718) used in this study were purchased from Abcam. The BeyoECL Plus (cat. no. P0018S, Beyotime) was used for the development of protein signals. The expression level of TLR4 was analyzed according to the densitometry analysis using Image Lab software (Bio-Rad).

## 2.9 Statistical analysis

The experiments were performed three times. Data were expressed as mean  $\pm$  standard deviation (S.D.). The comparison of more than two groups was conducted by ANOVA with Tukey's *post hoc* test. The difference between two groups was investigated by Student's *t*-test. Statistical analyses were conducted by

GraphPad Prism 7 software (GraphPad Inc., La Jolla, CA, USA) and  $P < 0.05$  was considered significant.

## 3. Results

### 3.1 XIST expression is elevated in ox-LDL-treated HUVECs

The atherogenic responses were developed using HUVECs stimulated via ox-LDL. As shown in figure 1A, cell viability was significantly inhibited by the treatment of ox-LDL for 24 h in a concentration dependent manner. Meanwhile, 50  $\mu$ g/ml ox-LDL induced viability suppression in a time dependent manner (figure 1B). Subsequently, HUVECs challenged with 50  $\mu$ g/ml ox-LDL for 24 h were used for the following experiments. The data of flow cytometry displayed that treatment of ox-LDL obviously led to apoptosis in HUVECs compared with control group (figure 1C), and induced cell arrest at S phase (supplementary figure 1). Moreover, the secretion levels of TNF- $\alpha$ , IL-6 and IL-1 $\beta$  in medium were markedly increased after the treatment of ox-LDL (figure 1D–F). In addition, the levels of ROS and MDA were significantly enhanced and SOD level was decreased in ox-LDL-treated HUVECs compared with those in control group (figure 1G–I). These findings indicated that exposure to ox-LDL induced viability inhibition, apoptosis promotion, inflammatory response and oxidative injury in HUVECs. XIST was a lncRNA associated with the damaged endothelial cells. To test the potential role of XIST in ox-LDL-induced HUVEC injury, its expression was measured in the cells. Results showed high expression of XIST in the treated cells (figure 1J). These results suggested that high expression of XIST might be associated with ox-LDL-induced injury in HUVECs.

### 3.2 Silence of XIST alleviates ox-LDL-induced HUVECs injury

To explore the biological role of XIST in ox-LDL-induced injury, HUVECs were transfected with si-XIST or si-NC and then stimulated with 50  $\mu$ g/ml ox-LDL for 24 h. As displayed in figure 2A, the expression level of XIST was significantly reduced in HUVECs after silence of XIST using siRNA. The silence of XIST rescued the viability of ox-LDL-treated cells (figure 2B). In addition, deficiency of XIST attenuated HUVECs apoptosis induced by ox-LDL (figure 2C). Moreover, knockdown of XIST mitigated the secretion levels of TNF- $\alpha$ , IL-6 and IL-1 $\beta$  in ox-

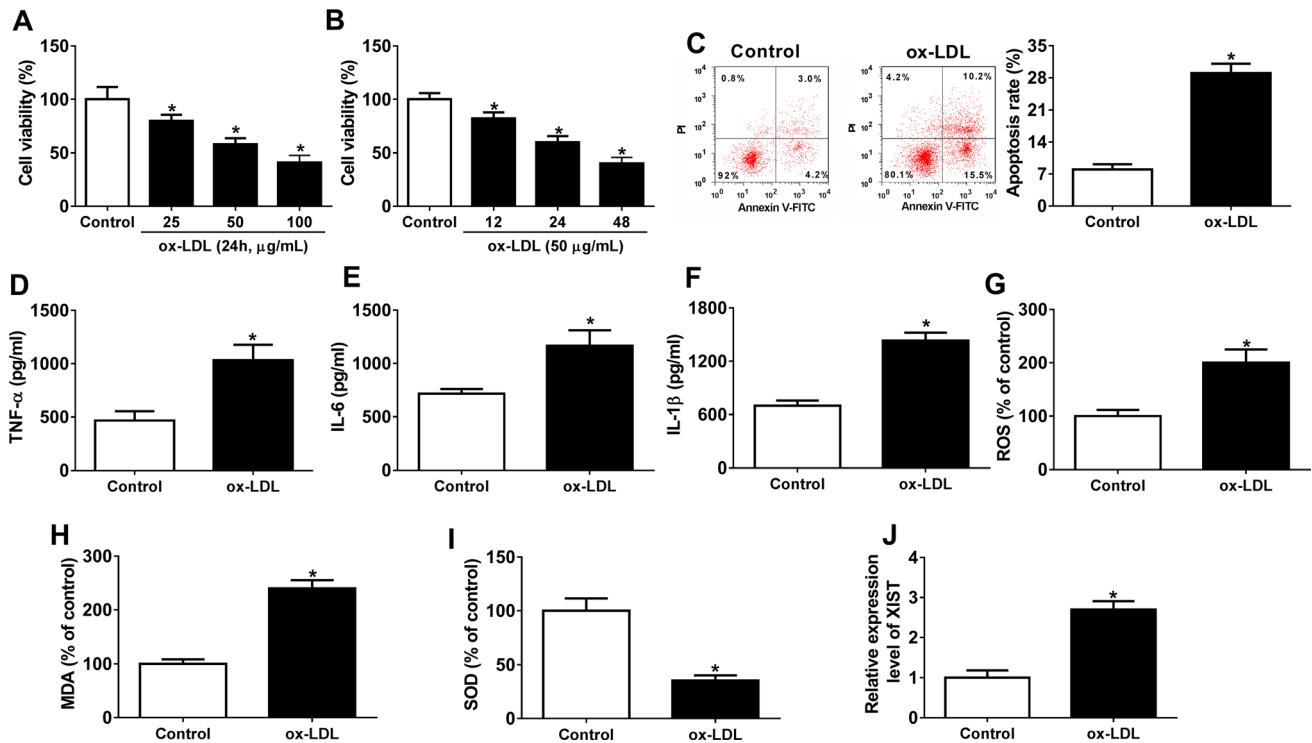


**Figure 1.** XIST expression is enhanced in ox-LDL-treated HUVECs. (A and B) Cell viability was measured in HUVECs after treatment of ox-LDL by MTT. (C) Cell apoptotic rate was measured in ox-LDL-treated HUVECs by flow cytometry. (D–F) The secretion levels of inflammatory cytokines were detected in ox-LDL-treated HUVECs by ELISA. (G–I) The levels of ROS, MDA and SOD were measured in HUVECs after treatment of ox-LDL by Reactive Oxygen Species Assay kit, Total Superoxide Dismutase Assay kit or Lipid Peroxidation MDA Assay kit, respectively. (J) The expression of XIST was measured in ox-LDL-treated HUVECs by qRT-PCR. \* $P < 0.05$ .

LDL-treated HUVECs (figure 2D–F). Besides, it was indicated in figure 2G–I that the levels of ROS and MDA in ox-LDL-challenged cells were greatly reduced by silence of XIST with the enhancement of SOD level. Furthermore, knockdown of XIST showed little effect on the viability, apoptosis, inflammatory response and oxidative stress in the un-treated HUVECs (supplementary figure 2A–I). These data uncovered that XIST knockdown could alleviate ox-LDL-induced HUVECs injury *in vitro*.

### 3.3 XIST directly targets miR-204-5p

To explore the underlying mechanism, bioinformatics analysis was performed to predict the targets of XIST using DIANA tool. We selected the 8 common atherogenic-associated miRNAs in the predictive targets, and found that miR-204-5p expression was decreased most via XIST overexpression or ox-LDL (supplementary figure 3A–C). The potential binding sites of miR-204-5p and XIST were displayed in figure 3A. The luciferase assay confirmed this prediction, showing the loss of luciferase activity in XIST WT group after transfection

of miR-204-5p mimic (figure 3B). Furthermore, miR-204-5p overexpression led to the increased level of XIST enriched by Ago2 RIP compared with miR-NC treatment, while IgG RIP exhibited little efficacy of enrichment (figure 3C). Additionally, the results of qRT-PCR demonstrated that the expression level of miR-204-5p was abnormally decreased in HUVECs after the treatment of ox-LDL (figure 3D). Moreover, the abundance of miR-204-5p was notably increased knockdown of by XIST and decreased by overexpression of XIST (figure 3E). These findings suggested XIST as a decoy of miR-204-5p.

### 3.4 Knockdown of miR-204-5p reverses silence of XIST-mediated injury inhibition in ox-LDL-treated HUVECs

To explore whether miR-204-5p was involved in XIST-mediated regulatory mechanism, HUVECs were transfected with si-NC, si-XIST, si-XIST + in-miR-NC or si-XIST + in-miR-204-5p before stimulation of ox-LDL. As indicated in figure 4A, the abundance of miR-204-5p was increased 2.65-fold by silence of XIST, while

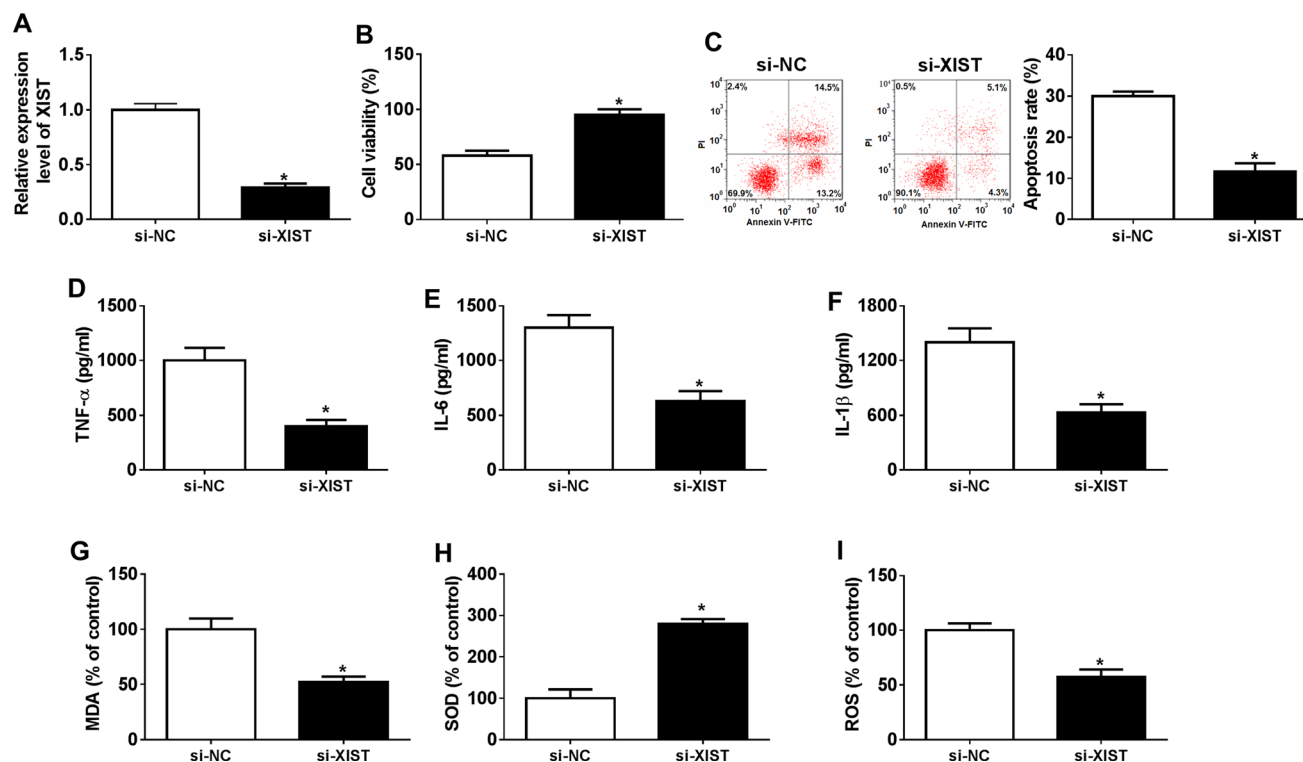


**Figure 2.** XIST knockdown inhibits ox-LDL-induced injury in HUVECs. HUVECs were transfected with si-XIST or si-NC and then treated with 50  $\mu$ g/ml ox-LDL for 24 h. The expression level of XIST (A), cell viability (B), apoptotic rate (C), inflammatory cytokines levels (D–F), ROS (G), MDA (H) and SOD (I) levels were detected in the treated HUVECs by qRT-PCR, MTT, flow cytometry, ELISA, Reactive Oxygen Species Assay kit, Total Superoxide Dismutase Assay kit or Lipid Peroxidation MDA Assay kit, respectively. \* $P < 0.05$ .

introduction of miR-204-5p inhibitor induced a 47% reduction of its level when compared with their corresponding control, respectively. Moreover, downregulation of miR-204-5p alleviated silence of XIST-mediated viability increase and apoptosis reduction in ox-LDL-treated HUVECs (figure 4B and C). Meanwhile, the data of ELISA assay showed that exhaustion of miR-204-5p attenuated the suppressive role of knockdown of XIST in secretion of TNF- $\alpha$ , IL-6 and IL-1 $\beta$  (figure 4D–F). In addition, the levels of ROS, MDA and SOD regulated by silence of XIST were restored by knockdown of miR-204-5p in the treated cells (figure 4G–I). These results indicated that XIST regulated ox-LDL-induced injury by sponging miR-204-5p.

### 3.5 TLR4 is a target of miR-204-5p

miRNAs functioned by targeting mRNA. Hence, bioinformatics analysis was performed by using DIANA tool, which provided the potential binding sites of miR-204-5p and TLR4 (figure 5A). To validate the interaction between miR-204-5p and TLR4, luciferase assay was conducted using wild-type and mutant

luciferase reporter vector targeting 3' UTR of TLR4. The results revealed that overexpression of miR-204-5p induced a 74% decrease of luciferase activity in TLR4 WT group, whereas it could not affect the activity in TLR4 MUT group (figure 5B). Moreover, after treatment of ox-LDL, HUVECs displayed higher level of TLR4 mRNA (figure 5C). Besides, the protein level of TLR4 was decreased 70% by overexpression of miR-204-5p and increased 3-fold by knockdown of miR-204-5p in HUVECs (figure 5D). Meanwhile, the data of western blot also revealed that TLR4 protein abundance was decreased 72% by silence of XIST and enhanced 3-fold via overexpression of XIST (figure 5E). These data showed TLR4 as a target of miR-204-5p.

### 3.6 miR-204-5p inhibits ox-LDL-induced injury by targeting TLR4 in HUVECs

To explore whether TLR4 was required for miR-204-5p-mediated injury regulation, HUVECs were transfected with miR-NC, miR-204-5p mimic, miR-204-5p mimic + pcDNA or miR-204-5p mimic + TLR4 overexpression vector before the stimulation of ox-

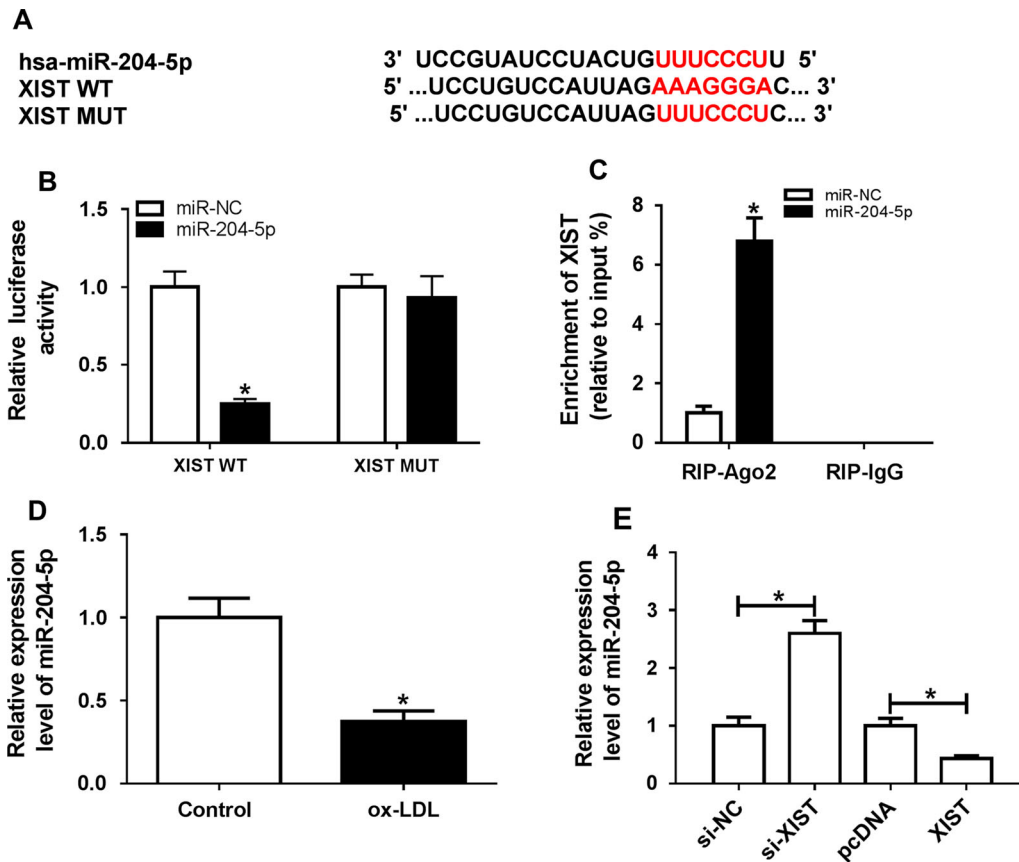


**Figure 3.** miR-204-5p is bound to XIST. (A) The binding sites of miR-204-5p and XIST were predicted by DIANA tool. (B) Luciferase assay was performed in HUVECs co-transfected with XIST WT or XIST MUT and miR-NC or miR-204-5p mimic. (C) Ago2 RIP assay was performed in HUVECs transfected with miR-204-5p mimic or miR-NC and XIST level were measured by qRT-PCR. (D) The expression of miR-204-5p was detected in HUVECs after treatment of ox-LDL by qRT-PCR. (E) The expression level of miR-204-5p was measured in HUVECs transfected with si-NC, si-XIST, pcDNA or XIST overexpression vector by qRT-PCR. \* $P < 0.05$ .

LDL. As displayed in figure 6A, the TLR4 protein level was greatly repressed by overexpression of miR-204-5p, which was restored by introduction of TLR4 overexpression vector. Moreover, overexpression of miR-204-5p increased cell viability and inhibited cell apoptosis, inflammatory response and oxidative stress caused by ox-LDL in HUVECs (figure 6B–I). However, this event was weakened by restoration of TLR4. Besides, the loss-of-function experiments confirmed that knockdown of TLR4 inhibited ox-LDL-induced injury in HUVECs (supplementary figure 4A–I). These results uncovered that miR-204-5p suppressed ox-LDL-induced injury by targeting TLR4.

### 3.7 XIST regulates TLR4 expression by competitively sponging miR-204-5p

To further elucidate the ceRNA network mediated by XIST, HUVECs were transfected with si-NC, si-XIST,

si-XIST + in-miR-NC or si-XIST + in-miR-204-5p. As demonstrated in figure 7A and 7B, the mRNA and protein levels of TLR4 were significantly decreased in HUVECs by silence of XIST, which was counteracted by deficiency of miR-204-5p. These findings suggested that XIST could regulate TLR4 expression by acting as a ceRNA for miR-204-5p.

## 4. Discussion

Ox-LDL is a key risk factor of atherosclerosis associated with the dysfunction of endothelial cells and thus HUVECs treated with ox-LDL were widely used as atherosclerosis model *in vitro* (Attanzio *et al.* 2019; Yin *et al.* 2019; Zhu *et al.* 2019). The secretion of inflammatory cytokines such as TNF- $\alpha$ , IL-6 and IL-1 $\beta$  is involved in the pathogenesis of atherosclerosis (Tousoulis *et al.* 2016). ROS plays an important role in the modulation of inflammatory response (Forrester

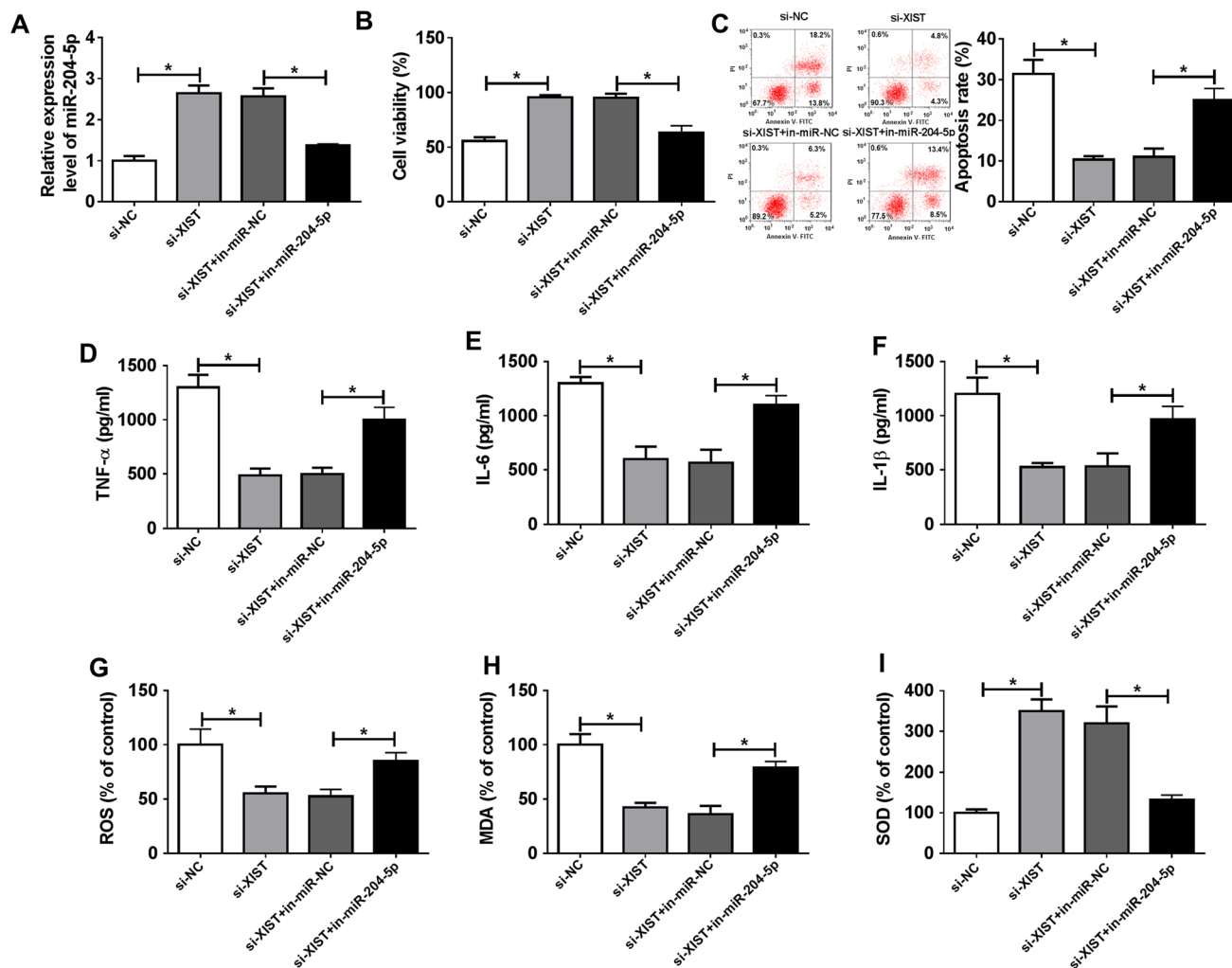


**Figure 4.** miR-204-5p deficiency reverses silence of XIST-mediated suppressive role in ox-LDL-induced HUVECs injury. HUVECs were transfected with si-NC, si-XIST, si-XIST + in-miR-NC or si-XIST + in-miR-204-5p and then treated with 50  $\mu$ g/ml ox-LDL for 24 h. The expression level of miR-204-5p (A), cell viability (B), apoptotic rate (C), inflammatory cytokines levels (D–F), ROS (G), MDA (H) and SOD (I) levels were detected in the treated HUVECs by qRT-PCR, flow cytometry, ELISA, Reactive Oxygen Species Assay kit, Total Superoxide Dismutase Assay kit or Lipid Peroxidation MDA Assay kit, respectively. \* $P < 0.05$ .

*et al.* 2018). Moreover, exposure to ox-LDL could induce oxidative stress and inflammatory injury in HUVECs (Zhu *et al.* 2019). In this study, after treatment of ox-LDL, cell apoptosis, inflammatory response and oxidative stress were induced in HUVECs, which were used as *in vitro* model of atherosclerosis. LncRNAs could serve as promising diagnostic and therapeutic tools for atherosclerosis (Zhang *et al.* 2018). In the present study, we found the up-regulated XIST in ox-LDL-induced HUVECs. Moreover, silence of XIST could competitively sponge miR-204-5p to reduce TLR4 expression, leading to the suppression of cell apoptosis, inflammatory response and oxidative stress in ox-LDL-treated HUVECs.

Previous work has suggested that knockdown of XIST could ameliorate ox-LDL-induced HUVECs apoptosis by regulating miR-320 and nucleotide-binding oligomerization domain 2 in atherosclerosis (Xu *et al.* 2018). Our work also revealed that silence of XIST suppressed ox-LDL-induced apoptosis. Moreover, inflammatory response and oxidative stress, as the key events in atherosclerosis, were repressed by interference of XIST. These results indicated the potential effect of inhibition of XIST on atherosclerosis. The ceRNA regulatory network is one major mechanism of lncRNA in the progression of cancers and diseases. It has been indicated that knockdown of XIST could alleviate inflammatory response by acting as a ceRNA



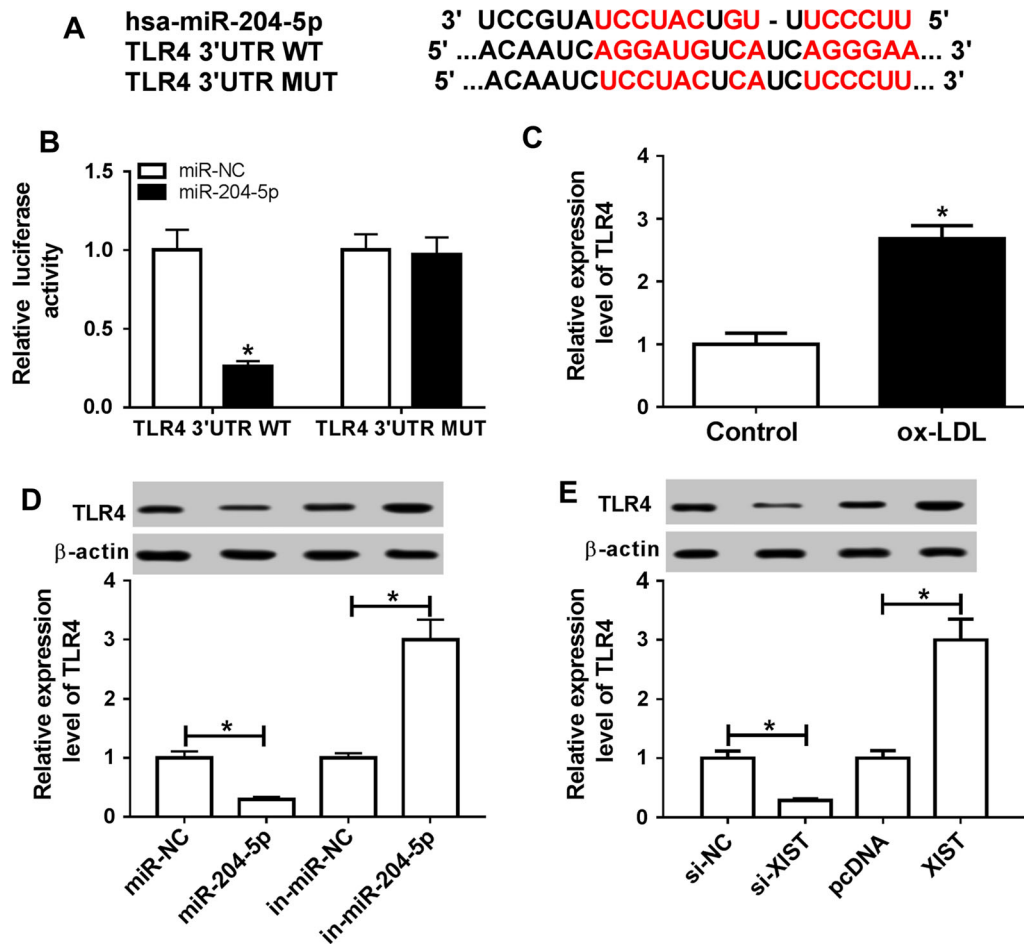


**Figure 5.** TLR4 is a target of miR-204-5p. (A) The binding sites of miR-204-5p and TLR4 were predicted by DIANA tool. (B) Luciferase assay was conducted in HUVECs co-transfected with TLR4 WT or TLR4 MUT and miR-NC or miR-204-5p. (C) The expression level of TLR4 mRNA was detected in HUVECs after exposure to ox-LDL by qRT-PCR. (D) The protein level of TLR4 was measured in HUVECs transfected with miR-NC, miR-204-5p mimic, in-miR-NC or in-miR-204-5p by western blot. (E) The expression level of TLR4 protein was measured in HUVECs transfected with si-NC, si-XIST, pcDNA or XIST overexpression vector by western blot. \* $P < 0.05$ .

for miR-544 or miR-146a (Jin *et al.* 2018; Sun *et al.* 2018). This paper first demonstrated XIST as a sponge of miR-204-5p, which was confirmed by luciferase assay and RIP assay.

Previous study showed that miR-204-5p could inhibit apoptosis, inflammatory response and oxidative stress in lipopolysaccharide-treated rat mesangial cells (Chen *et al.* 2018). In the present study, we also found the anti-apoptotic and anti-inflammatory role of miR-204-5p in ox-LDL-treated HUVECs, which is similar to former work (Yan *et al.* 2019). Besides, the results also revealed the anti-oxidative effect of miR-204-5p overexpression by decreasing ROS and MDA and increasing SOD levels. Meanwhile, knockdown of miR-204-5p attenuated the protective effect of silence

of XIST on ox-LDL-induced injury, uncovering that XIST might regulate atherogenesis progression by sponging miR-204-5p. Function of miRNA is usually realized by targeting 3' UTR sequences of mRNA. This research first provided TLR4 as a functional target of miR-204-5p, which was confirmed by luciferase assay.

TLR4 expression was enhanced in HUVECs after treatment of ox-LDL, which is consistent with previous studies (Qin *et al.* 2018; Tian *et al.* 2018; Yang and Gao 2019). In addition, these reports suggested that TLR4 could contribute to atherogenesis progression by promoting ox-LDL-induced endothelial cell apoptosis, inflammatory response and oxidative stress (Qin *et al.* 2018; Tian *et al.* 2018; Yang and Gao 2019). In this study, we also found the promoting role of TLR4 in

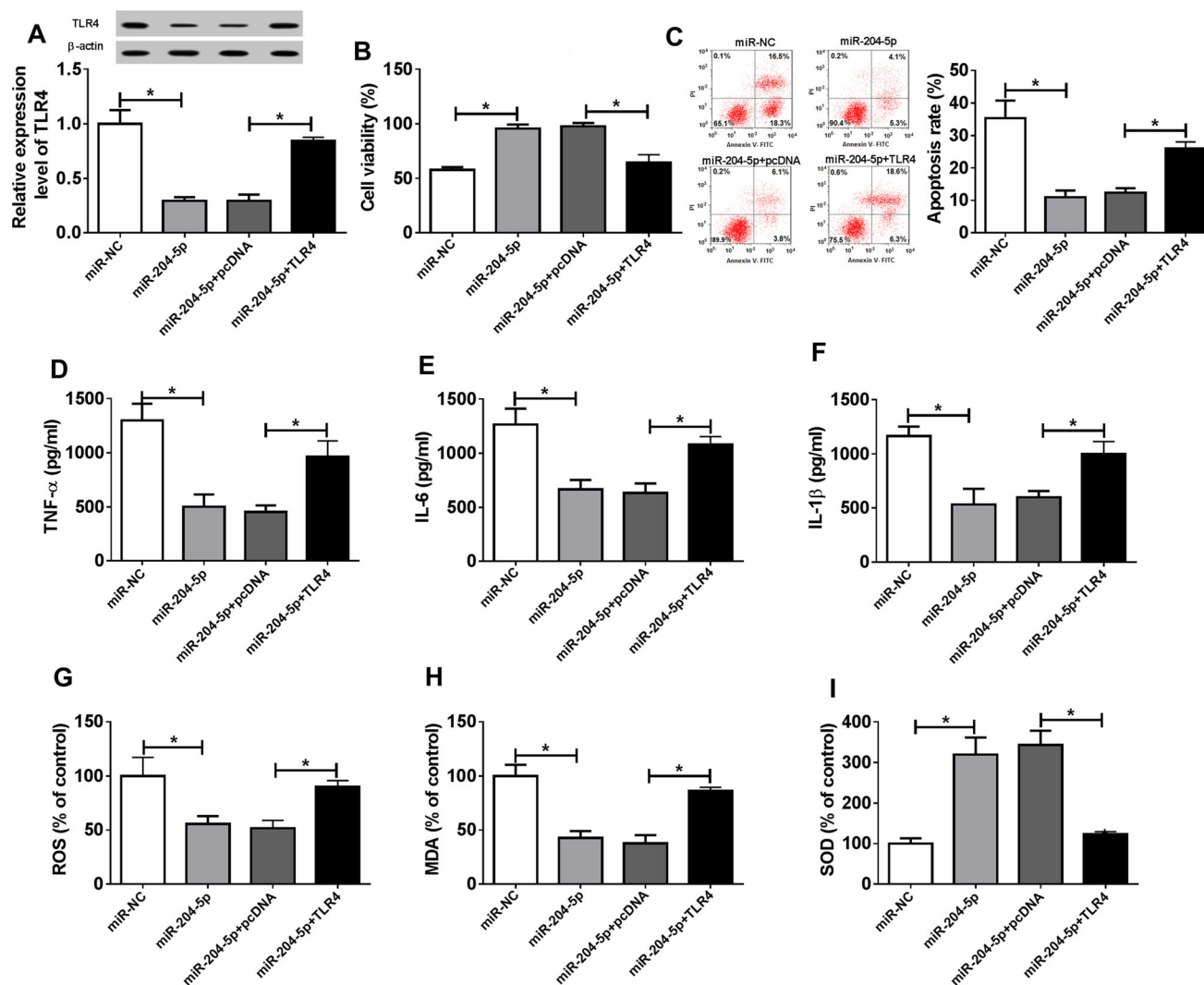


**Figure 6.** TLR4 attenuates miR-204-5p-mediated suppressive role in ox-LDL-induced HUVECs injury. HUVECs were transfected with miR-NC, miR-204-5p mimic, miR-204-5p mimic + pcDNA or miR-204-5p mimic + TLR4 overexpression vector and then treated with 50  $\mu$ g/ml ox-LDL for 24 h. TLR4 protein level (A), cell viability (B), apoptotic rate (C), inflammatory cytokines levels (D–F), ROS (G), MDA (H) and SOD (I) levels were detected in the treated HUVECs by western blot, MTT, flow cytometry, ELISA, Reactive Oxygen Species Assay kit, Total Superoxide Dismutase Assay kit or Lipid Peroxidation MDA Assay kit, respectively. \* $P < 0.05$ .

atherogenesis by weakening the suppressive role of miR-204-5p in ox-LDL-induced injury. Moreover, TLR4 mRNA and protein levels were decreased by knockdown of XIST in HUVECs, which is also in agreement with former work (Jin *et al.* 2019). Furthermore, miR-204-5p deficiency abrogated this effect, indicating that XIST could target TLR4 expression by competitively sponging miR-204-5p in HUVECs. To better understand the mechanism of atherogenesis, we plan to use an ApoE<sup>-/-</sup> mice model of atherogenesis (Cheng *et al.* 2018) to investigate the function of XIST *in vivo* in further study. The role of XIST is exhibited in

the inactivated X-chromosome of females and is silent in males. Hence, we hypothesized that there were other promising mechanisms for the development of atherogenesis in males, which should be explored in future.

In conclusion, here we indicated the promoting role of XIST in ox-LDL-induced HUVECs injury. Knockdown of XIST attenuated ox-LDL-induced inhibition of viability and promotion of apoptosis, inflammatory response and oxidative stress in HUVECs, possibly by acting as a ceRNA for miR-204-5p to target TLR4. These findings may provide a novel mechanism for understanding the pathogenesis of atherogenesis.

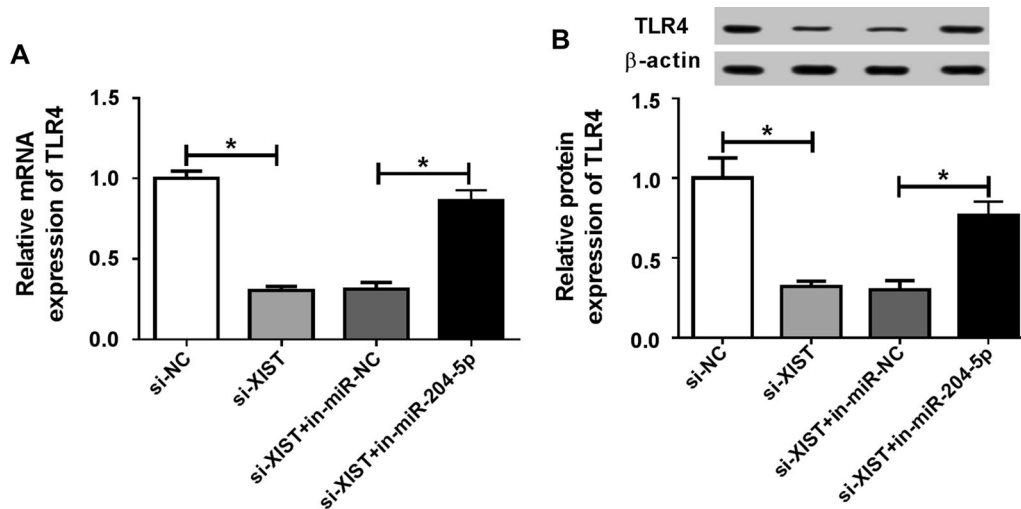


**Figure 7.** TLR4 expression is regulated by XIST and miR-204-5p. (A and B) The expression levels of TLR4 mRNA and protein were measured in HUVECs transfected with si-NC, si-XIST, si-XIST + in-miR-NC or si-XIST + in-miR-204-5p by qRT-PCR and western blot. \* $P < 0.05$ .

## References

- Aryal B and Suarez Y 2019 Non-coding RNA regulation of endothelial and macrophage functions during atherosclerosis. *Vasc. Pharmacol.* **114** 64–75
- Attanzio A, Frazzitta A, Busa R, Tesoriere L, Livrea MA and Allegra M 2019 Indicaxanthin from opuntia ficus indica (L. Mill) inhibits oxidized LDL-mediated human endothelial cell dysfunction through inhibition of NF-kappaB activation. *Oxid. Med. Cell Longev.* **2019** 3457846
- Chen Y, Qiu J, Chen B, Lin Y, Chen Y, Xie G, Qiu J, Tong H, *et al.* 2018 Long non-coding RNA NEAT1 plays an important role in sepsis-induced acute kidney injury by targeting miR-204 and modulating the NF-kappaB pathway. *Int. Immunopharmacol.* **59** 252–260
- Cheng S, Zhou F, Xu Y, Liu X, Zhang Y, Gu M, Su Z, Zhao D, *et al.* 2018 Geniposide regulates the miR-101/MKP-1/p38 pathway and alleviates atherosclerosis inflammatory injury in ApoE(-/-) mice. *Immunobiology* **224** 296–306
- den Dekker WK, Cheng C, Pasterkamp G and Duckers HJ 2010 Toll like receptor 4 in atherosclerosis and plaque destabilization. *Atherosclerosis* **209** 314–320
- Fasanaro P, Greco S, Lorenzi M, Pescatori M, Brioschi M, Kulshreshtha R, Banfi C, Stubbs A *et al.* 2009 An integrated approach for experimental target identification of hypoxia-induced miR-210. *J. Biol. Chem.* **284** 35134–35143
- Forrester SJ, Kikuchi DS, Hernandez MS, Xu Q and Griendling KK 2018 Reactive oxygen species in metabolic and inflammatory signaling. *Circ. Res.* **122** 877–902
- Haybar H, Shahrabi S, Rezaeeyan H, Shirzad R and Saki N 2019 Endothelial cells: from dysfunction mechanism to pharmacological effect in cardiovascular disease. *Cardio-vasc. Toxicol.* **19** 13–22
- Hennessy EJ, Parker AE and O'Neill LA 2010 Targeting toll-like receptors: emerging therapeutics? *Nat. Rev. Drug Discov.* **9** 293–307
- Islas JF and Moreno-Cuevas JE 2018 A MicroRNA perspective on cardiovascular development and diseases: an update. *Int. J. Mol. Sci.* **19** 2075
- Jin H, Du XJ, Zhao Y and Xia DL 2018 XIST/miR-544 axis induces neuropathic pain by activating STAT3 in a rat model. *J. Cell Physiol.* **233** 5847–5855
- Jin LW, Pan M, Ye HY, Zheng Y, Chen Y, Huang WW, Xu XY and Zheng SB 2019 Down-regulation of the long non-coding RNA XIST ameliorates podocyte apoptosis in membranous nephropathy via the miR-217-TLR4 pathway. *Exp. Physiol.* **104** 220–230
- Li S, Sun Y, Zhong L, Xiao Z, Yang M, Chen M, Wang C, Xie X *et al.* 2018 The suppression of ox-LDL-induced inflammatory cytokine release and apoptosis of HCAECs by long non-coding RNA-MALAT1 via regulating microRNA-155/SOCS1 pathway. *Nutr. Metab. Cardio-vasc. Dis.* **28** 1175–1187
- Liang W, Fan T, Liu L and Zhang L 2019 Knockdown of growth-arrest specific transcript 5 restores oxidized low-density lipoprotein-induced impaired autophagy flux via upregulating miR-26a in human endothelial cells. *Eur. J. Pharmacol.* **843** 154–161
- Liu JL, Zhang WQ, Zhao M and Huang MY 2019 Upregulation of long noncoding RNA XIST is associated with poor prognosis in human cancers. *J. Cell Physiol.* **234** 6594–6600
- Livak KJ and Schmittgen TD 2001 Analysis of relative gene expression data using real-time quantitative PCR and the 2(-Delta Delta C(T)) method. *Methods* **25** 402–408

- Neumann P, Jaé N, Knau A, Glaser SF, Fouani Y, Rossbach O, Krüger M, John D, et al. 2018 The lncRNA GATA6-AS epigenetically regulates endothelial gene expression via interaction with LOXL2. *Nat. Commun.* **9** 237
- Pothineni NVK, Subramany S, Kuriakose K, Shirazi LF, Romeo F, Shah PK and Mehta JL 2017 Infections, atherosclerosis, and coronary heart disease. *Eur. Heart J.* **38** 3195–3201
- Qin SB, Peng DY, Lu JM and Ke ZP 2018 MiR-182-5p inhibited oxidative stress and apoptosis triggered by oxidized low-density lipoprotein via targeting toll-like receptor 4. *J. Cell Physiol.* **233** 6630–6637
- Singh KK, Matkar PN, Pan Y, Quan A, Gupta V, Teoh H, Al-Omran M and Verma S 2017 Endothelial long non-coding RNAs regulated by oxidized LDL. *Mol. Cell Biochem.* **431** 139–149
- Sun W, Ma M, Yu H and Yu H 2018 Inhibition of lncRNA X inactivate-specific transcript ameliorates inflammatory pain by suppressing satellite glial cell activation and inflammation by acting as a sponge of miR-146a to inhibit Nav 1.7. *J. Cell Biochem.* **119** 9888–9898
- Tian D, Sha Y, Lu JM and Du XJ 2018 MiR-370 inhibits vascular inflammation and oxidative stress triggered by oxidized low-density lipoprotein through targeting TLR4. *J. Cell Biochem.* **119** 6231–6237
- Tousoulis D, Oikonomou E, Economou EK, Crea F and Kaski JC 2016 Inflammatory cytokines in atherosclerosis: current therapeutic approaches. *Eur. Heart J.* **37** 1723–1732
- Trpkovic A, Resanovic I, Stanimirovic J, Radak D, Mousa SA, Cenic-Milosevic D, Jevremovic D and Isenovic ER 2015 Oxidized low-density lipoprotein as a biomarker of cardiovascular diseases. *Crit. Rev. Clin. Lab. Sci.* **52** 70–85
- Wei M, Li L, Zhang Y, Zhang ZJ, Liu HL and Bao HG 2019 LncRNA X inactive specific transcript contributes to neuropathic pain development by sponging miR-154-5p via inducing toll-like receptor 5 in CCI rat models. *J. Cell Biochem.* **120** 1271–1281
- Xu X, Ma C, Liu C, Duan Z and Zhang L 2018 Knockdown of long noncoding RNA XIST alleviates oxidative low-density lipoprotein-mediated endothelial cells injury through modulation of miR-320/NOD2 axis. *Biochem. Biophys. Res. Commun.* **503** 586–592
- Yan L, Liu Z, Yin H, Guo Z and Luo Q 2019 Silencing of MEG3 inhibited ox-LDL-induced inflammation and apoptosis in macrophages via modulation of the MEG3/miR-204/CDKN2A regulatory axis. *Cell Biol. Int.* **43** 409–420
- Yang L and Gao C 2019 MiR-590 inhibits endothelial cell apoptosis by inactivating the TLR4/NF-kappaB pathway in atherosclerosis. *Yonsei Med. J.* **60** 298–307
- Yin J, Hou X and Yang S 2019 microRNA-338-3p promotes ox-LDL-induced endothelial cell injury through targeting BAMBI and activating TGF-beta/Smad pathway. *J. Cell Physiol.* **234** 11577–11586
- Yuan T, Yang T, Chen H, Fu D, Hu Y, Wang J, Yuan Q, Yu H, et al. 2019 New insights into oxidative stress and inflammation during diabetes mellitus-accelerated atherosclerosis. *Redox. Biol.* **20** 247–260
- Zhang Z, Salisbury D and Sallam T 2018 Long noncoding RNAs in atherosclerosis: JACC review topic of the week. *J. Am. Coll. Cardiol.* **72** 2380–2390
- Zhu Z, Li J and Zhang X 2019 Astragaloside IV protects against oxidized low-density lipoprotein (ox-LDL)-induced endothelial cell injury by reducing oxidative stress and inflammation. *Med. Sci. Monit.* **25** 2132–2140

Corresponding editor: ULLAS KOLTHUR-SEETHARAM